NASA CR-132453

DEVELOPMENT OF A METHOD OF ANALYSIS AND COMPUTER PROGRAM FOR CALCULATING THE INVISCID FLOW ABOUT THE WINDWARD SURFACES OF SPACE SHUTTLE CONFIGURATIONS AT LARGE ANGLES OF ATTACK

By Stephen H. Maslen

January 1974

MML TECHNICAL REPORT TR 74-5c

Final Report

Prepared under Contract No. NAS1-11604 by

Martin Marietta Corporation
Martin Marietta Laboratories (Formerly RIAS)
1450 South Rolling Road
Baltimore, Maryland 21227

for

NATIONAL AERONAUTICS AND SPACE ADMINISTRATION
Langley Research Center

NASA CR - 132453

DEVELOPMENT OF A METHOD OF ANALYSIS AND COMPUTER PROGRAM FOR CALCULATING THE INVISCID FLOW ABOUT THE WINDWARD SURFACES OF SPACE SHUTTLE CONFIGURATIONS AT LARGE ANGLES OF ATTACK

By Stephen H. Maslen

January 1974

MML Technical Report TR 74-5c

Final Report

Prepared under Contract No. NAS1-11604 by
Martin Marietta Corporation
Martin Marietta Laboratories (Formerly RIAS)
1450 South Rolling Road
Baltimore, Maryland 21227

for

National Aeronautics and Space Administration

Langley Research Center

INVISCID THREE-DIMENSIONAL HYPERSONIC FLOW AT LARGE ANGLES OF ATTACK

By S. H. Maslen
Martin Marietta Laboratories
Martin Marietta Corporation

SUMMARY

A general method developed for the analysis of inviscid hypersonic shock layers is discussed for application to the case of the shuttle vehicle at high (65°) angle of attack. The associated extensive subsonic flow region caused convergence difficulties whose resolution is discussed. It is required that the solution be smoother than anticipated.

INTRODUCTION

The supply of solutions for the inviscid flow in a shock layer, such as that about a blunted body moving at hypersonic speeds, is very large and it might appear that another such method would be, to say the least, superfluous. However the goals of this work are special. The aim is to find an efficient and economical solution for the shock layer on the windward side of the shuttle vehicle at 65° angle of attack. An exact analysis is not sought but only a reliable one. Thus the precise time-dependent methods or even the method of characteristics are rejected because of the required computing time. On the other hand, Newtonian methods are simple but do not provide the desired detail in the shock layer.

Some time ago Maslen (ref. 1) proposed a method for axisymmetric flow based on the use of a Mises transformation coupled with a simple approximate integral of the lateral (to the shock) momentum equations. A number of solutions were given and the results were indeed accurate and very easy to obtain.

The simplicity of the method led several others to apply the method to elaborations of the original case. Jackson (ref. 2) considered viscous effects and also used the method to solve the complete equations of motion iteratively. Perini and Melnik (ref. 3) solved nonequilibrium flow, while Olstad (ref. 4) applied the procedure to radiating flow and to the massive blowing problem associated with extreme heating rates. Recently, Grose (ref. 5) has presented detailed solutions for nonequilibrium hypersonic flows for a variety of cases of interest in planetary entry.

Subsequently, Maslen (ref. 6) returned to the original inviscid equilibrium flow case, but considered general three-dimensional geometry. None of the elaborations mentioned above were examined. However the basic analysis was presented for a general smooth three-dimensional geometry. The present study is an extension of that analysis to the specific case cited above, the windward surface of the shuttle vehicle at high angle of attack.

SYMBOLS

a, b, c	shock curvature functions, eq. (35)
$\bar{a}, \bar{b}$	constants, eq. (36)
A, B, D, E	auxiliary functions, eq. (5) or eq. (22)
c	speed of sound behind shock
h	enthalpy
L	differential operator, eq. (7)
M_∞	free stream Mach number
P	pressure
P_1, P_2	pressure functions, eqs. (19), (20)
S	entropy
u_1, v_1, w_1	velocity components, cylindrical coordinates
$U, \bar{V}$	velocity components, defined in eqs. (2)
x, r, ω	cylindrical coordinates, fig. 1
x_1, r_1, w_1	cylindrical coordinates (wind axes)
z	shock layer coordinate, fig. 1, and eq. (1)
α	angle of attack
β	auxiliary function, eq. (28)
γ	ratio of specific heats
Δ	auxiliary function, eq. (5)
η	shock layer coordinate, fig. 1 and eq. (1)

ζ	"Mises" type coordinate, eq. (6)
θ	shock layer coordinate, fig. 1 and eq. (1)
λ	$\mathrm{Tan}^{-1}\left(\frac{1}{r}\frac{\partial r}{\partial \theta}\right)_s$, fig. 1
ν	$\mathrm{Tan}^{-1}\left(\partial r/\partial z\right)_s$, fig. 1
ξ	flow angle, eq. (2)
ρ	density
σ	"Mises" type coordinate, eq. (6)
τ	$\mathrm{Tan}^{-1}\left(\mathrm{Tan}\ \nu\ \mathrm{Cos}\ \lambda\right)$, fig. 1
φ	stream function, eq. (3)
ψ	stream function, eq. (3), also "Mises" type coordinate, eq. (6)

Subscripts:

s	shock value
∞	free stream value
x, r, w z, η, θ ζ, σ, ψ	partial derivative

GENERAL ANALYSIS

The equation to be solved are the inviscid Euler equations for steady, compressible, isoenergetic flow. The development of the appropriate approximate system actually solved is discussed in reference 6 and the following is a summary of the development in that report.

Consider a set of coordinates (z, η, θ) related to the flow geometry (Fig. 1). We base them on the shock where z, θ are the axial and azimuthal coordinates of a point on the shock while η is the (normal) distance from shock to field point. These coordinates are related to cylindrical ones (x, r, ω) by

$$x = z + \eta \text{ Sin } \tau$$

$$r^2 = r_s^2 + \eta^2 \text{ Cos}^2 \tau - 2\eta r_s \text{ Cos } \tau \text{ Cos } \lambda \tag{1}$$

$$r \text{ Sin } (\omega-\theta) = \eta \text{ Cos } \tau \text{ Sin } \lambda$$

where $r_s = r_s(z,\theta)$ is the equation of the shock and ν, λ, and τ are angles defined in the symbol list. Now introduce three mutually perpendicular velocity components, U, $\bar{V}$ Cos ξ, $\bar{V}$ Sin ξ where U is normal to the shock and ξ is otherwise arbitrarily chosen. Then

$$U = u_1 \text{ Sin } \tau - v_1 \text{ Cos } \tau \text{ Cos } (\omega-\theta+\lambda) + w_1 \text{ Cos } \tau \text{ Sin } (\omega-\theta+\lambda)$$

$$\bar{V} \text{ Cos } \xi = u_1 \text{ Cos } \tau + v_1 \text{ Sin } \tau \text{ Cos } (\omega-\theta+\lambda) - w_1 \text{ Sin } \tau \text{ Sin } (\omega-\theta+\lambda) \tag{2}$$

$$\bar{V} \text{ Sin } \xi = - v_1 \text{ Sin } (\omega-\theta+\lambda) - w_1 \text{ Cos } (\omega-\theta+\lambda)$$

The Euler equations can be solved by the introduction of a pair of stream functions, ψ and φ, such that

$$\rho\vec{U} = \vec{\nabla}\psi \times \vec{\nabla}\varphi \tag{3}$$

or

$$\rho r U = (\psi_z \varphi_\theta - \psi_\theta \varphi_z)/\Delta$$

$$\rho\bar{V}(D\text{Cos}\,\xi + E \text{ Sin } \xi) = \psi_\eta \varphi_z - \varphi_\eta \psi_z \tag{4}$$

$$\rho\bar{V}(A\text{Cos}\,\xi + B \text{ Sin } \xi) = \frac{1}{r}(\psi_\theta \varphi_\eta - \psi_\eta \varphi_\theta)$$

where A, B, D, E and Δ are geometric factors given by

$$A = [r_s + \eta \text{ Cos } \tau \text{ Cos } \lambda \ (\lambda_\theta - 1)]/r \text{ Cos } \lambda$$

$$B = \frac{\eta}{r} r_\theta \tag{5}$$

$$D = \text{Tan } \tau \text{ Tan } \lambda + \eta\lambda_z \text{ Cos } \tau$$

$$E = (1 + \eta r_z \text{ Cos } \tau)/\text{Cos } \tau$$

$$\Delta = AE - BD$$

Now introduce a final coordinate system. This is a sort of Mises transformation in which we interchange ψ and η as dependent and independent variables. The specific use will clearly depend on the way in which ψ and σ (eq. (3)) are subsequently chosen. Let the new independent variables be ψ, ζ, σ

where

$$\begin{aligned} \zeta &= z \\ \sigma &= \theta \\ \psi &= \psi(\eta, z, \theta) \end{aligned} \tag{6}$$

Further, define the operator L by

$$L = -\frac{(D \cos\xi + E \sin\xi)}{r}\frac{\partial}{\partial \sigma} + (A \cos\xi + B \sin\xi)\frac{\partial}{\partial \zeta} \tag{7}$$

Then equations (4) yield, noting (5)

$$L(\varphi) = 0 \tag{8}$$

$$\bar{V} L(\eta) = U(AE-BD) \tag{9}$$

$$\rho \bar{V} \eta_\psi = \frac{-\varphi_\sigma}{r(A \cos\xi + B \sin\xi)} = \frac{-\varphi_\xi}{D \cos\xi + E \sin\xi} \tag{10}$$

The energy equation becomes

$$L(S) = 0 \tag{11}$$

while the isoenergetic condition is

$$h + \frac{1}{2}(U^2 + \bar{V}^2) = \text{constant} \tag{12}$$

The momentum equations become

$$-\Delta \frac{P_\psi}{\eta_\psi} = \rho \bar{V} [L(U) - \bar{V} \cos\xi L(\tau) + \bar{V} \sin\xi \cos\tau L(\lambda)-\theta)] \tag{13}$$

$$- [A(P_\zeta - P_\psi \eta_\zeta/\eta_\psi) - \frac{D}{r}(P_\sigma - P_\psi \eta_\sigma/\eta_\psi)] \tag{14}$$

$$= \rho\bar{V}[L(\bar{V}\ \mathrm{Cos}\ \xi) + UL(\tau) - \bar{V}\ \mathrm{Sin}\ \xi\ \mathrm{Sin}\ \tau\ L(\lambda-\theta)]$$

$$- [B(P_\zeta - P_\psi \eta_\zeta/\eta_\psi) - \frac{E}{r}(P_\sigma - P_\psi \eta_\sigma/\eta_\psi)] \tag{15}$$

$$= \rho\bar{V}[L(\bar{V}\ \mathrm{Sin}\ \xi) + (\bar{V}\ \mathrm{Cos}\ \xi\ \mathrm{Sin}\ \tau - U\ \mathrm{Cos}\ \tau)\ L(\lambda-\theta)]$$

These last three equations can be combined to give the Bernoulli relation

$$L(P) + \frac{\rho}{2} L(U^2 + \bar{V}^2) = 0 \tag{16}$$

The equations to be solved then consist of (8), (9), (10), (11), (12), any two of (13)-(16) and a state relation. The dependent variables are the three velocity components (U, $\bar{V}$, ξ), the thermodynamic variables (P, ρ, S, h), one physical coordinate (η), and one stream function (Ψ).

For later use, we will need the values of P_ψ at the shock. After some labor

$$\frac{P_\psi}{\rho\eta_\psi} = \bar{V}^2 \mathrm{Cos}\ \tau\ \mathrm{Cos}\ \lambda[\mathrm{Cos}\ \xi\ L(\tau) - \mathrm{Sin}\ \xi\ \mathrm{Cos}\ \tau\ L(\lambda-\theta)] \left\{\frac{1 - \dfrac{dU}{U_\infty d\mathrm{Sin}\ \beta} + \dfrac{U}{\rho U_\infty c^2}\dfrac{dP}{d\mathrm{Sin}\ \beta}}{1 - U^2/c^2}\right\} \tag{17}$$

$$- \frac{\rho U^2}{\rho_\infty}\left[\tau_z \mathrm{Cos}\ \tau - \frac{\mathrm{Cos}\ \tau\ \mathrm{Cos}\ \lambda}{r}(1-\lambda_\theta) - \frac{\mathrm{Sin}\ \tau\ \mathrm{Sin}\ \lambda\ \tau_\theta}{r}\right]\left\{\frac{1 - \rho_\infty/\rho}{1 - U^2/c^2}\right\}$$

where c is the speed of sound behind the shock. Note that all the derivatives on the right side lie along the shock since, clearly, ζ and σ in the operator L as used here can be replaced by z, θ.

As discussed in reference 6, we now approximate the momentum equation normal to the shock (eq. (13)) by its value at the shock, eq. (17), setting the terms in curly brackets equal to unity and assuming that the second line varies linearly with ψ across the shock. In that case one obtains

$$P(\psi,\zeta,\sigma) = P_s(\zeta,\sigma) + P_1(\zeta,\sigma)(\psi - \psi_s) - P_2(\zeta,\sigma)\left(\frac{\psi^2 - \psi_s^2}{2\psi_s}\right) \tag{18}$$

where

$$P_1 = \left\{\eta_\psi \rho \bar{V}^2 \operatorname{Cos}\tau \operatorname{Cos}\lambda \left[\operatorname{Cos}\xi\, L(\tau) - \operatorname{Sin}\xi \operatorname{Cos}\tau\, L(\lambda-\theta)\right]\right\}_s \tag{19}$$

and

$$P_2 = \left\{\eta_\psi \rho\left(\frac{\rho}{\rho_{oo}}\right)U^2 \left[\operatorname{Cos}\tau\, \tau_z - \operatorname{Cos}\tau \operatorname{Cos}\lambda\,(1-\lambda_\theta)/r - \operatorname{Sin}\tau \operatorname{Sin}\lambda\, \tau_\theta / r\right]\right\}_s \tag{20}$$

Finally, eq. (12) can be closely approximated as

$$h + \frac{\bar{V}^2}{2} = \text{constant} \tag{21}$$

while equations (7), (8) and (11) are applied, but setting $\eta = 0$ in A, B, D, E. Thus, we have

$$\begin{aligned} A &= 1/\operatorname{Cos}\lambda \\ B &= 0 \\ D &= \operatorname{Tan}\tau \operatorname{Tan}\lambda \\ E &= 1/\operatorname{Cos}\tau \end{aligned} \tag{22}$$

Then neglecting u and η, the two momentum equations (14) and (15) can be combined to yield

$$\rho\bar{V}^2\left[L(\xi) + \operatorname{Sin}\tau\, L(\lambda - \theta)\right] = A \operatorname{Sin}\xi\, P_\zeta + (E \operatorname{Cos}\xi - D \operatorname{Sin}\xi)\frac{P_\sigma}{r} \tag{23}$$

Finally, from eq. (7), the equation for the streamlines is

$$\frac{d\sigma}{d\zeta} = \frac{-(DV + EW)}{r(AV + BW)} \tag{24}$$

while along the streamlines, eq. (23) becomes

$$\frac{d \sin \xi}{d\zeta} = \frac{1}{\rho \bar{V}^2} \left\{ \sin \xi \left(P_\zeta - \frac{\tan \tau \sin \lambda}{r} P_\sigma \right) + \frac{\cos \xi \cos \lambda}{r \cos \tau} P_\sigma \right\}$$
$$+ \sin \xi \left[\frac{\cos \lambda \tan \tau \ (\lambda_\theta - 1)}{r} \right] - \frac{\cos \xi \cos \lambda \tan \tau}{r \cos \tau} \tau_\theta \qquad (25)$$

Equations (18), (21), (8), (11) and (25) plus a state equation are a complete system of equations for P, ρ, h, S, ϕ, $\bar{V}$ and ξ. The only differential operator appearing is L (eq. (7)) which is the ordinary derivative along a streamline.

After the system is solved, the solution is completed by returning to the physical (z, θ, η) space via eq. (10). Experience in the axisymmetric case has shown that it is preferable to evaluate eq. (10) exactly without making the small η approximation of eqs. (22).

Boundary Conditions

In the free stream, we set

$$\varphi = \omega_1 = \tan^{-1} \left[\frac{r \sin \omega \cos \alpha - x \sin \alpha}{r \cos \omega} \right] \qquad (26)$$

$$\psi = \frac{\rho_\infty U_\infty r_1^2}{2} = \frac{\rho_\infty U_\infty}{2} \left[(r \cos \omega)^2 + (r \sin \omega \cos \alpha - x \sin \alpha)^2 \right]$$
$$= \frac{\rho_\infty U_\infty}{2} \left[\frac{r \cos \omega}{\cos \varphi} \right]^2 \qquad (27)$$

where x_1, r_1, ω_1, are cylindrical coordinates aligned on wind axis. Equations Equations (26) and (27) are consistent with eq. (3) in the uniform free stream and, for axial symmetry, ψ is simply the usual Stokes stream function. The shock is taken to be Rankine-Hugoniot. The quantitites ρU, $\bar{V}$, ξ, ϕ, ψ and $\rho \eta_\psi$ are continuous across it. Thus, immediately behind the shock

$$\rho U/\rho_\infty U_\infty = \text{Sin}\,\tau\,\text{Cos}\,\alpha - \text{Cos}\,\tau\,\text{Sin}\,\alpha\,\text{Sin}(\theta-\lambda) \equiv \text{Sin}\,\beta \tag{28}$$

$$\bar{V}\,\text{Cos}\,\xi/U_\infty = \text{Cos}\,\tau\,\text{Cos}\,\alpha + \text{Sin}\,\tau\,\text{Sin}\,\alpha\,\text{Sin}\,(\theta-\lambda) \tag{29}$$

$$\bar{V}\,\text{Sin}\,\xi/U_\infty = -\text{Sin}\,\alpha\,\text{Cos}\,(\theta-\lambda) \tag{30}$$

$$\varphi = \text{Tan}^{-1}\left[\frac{r_s\,\text{Sin}\,\theta\,\text{Cos}\alpha - z\,\text{Sin}\,\alpha}{r_s\,\text{Cos}\,\theta}\right] \tag{31}$$

$$1/\eta_\psi = \rho U_\infty \{z(\text{Sin}\,\tau - \text{Cos}\,\alpha\,\text{Sin}\,\beta) - r\,(\text{Cos}\,\tau\,\text{Cos}\,\lambda + \text{Sin}\,\theta\,\text{Sin}\,\alpha\,\text{Sin}\,\beta)\} \tag{32}$$

where Sin β is defined by eq. (28). Clearly, β is the complement of the angle between the wind direction and the normal to the shock so that the Mach number normal to the shock is M_∞ Sin β. The Rankine Hugoniot relations yield

$$P/P_\infty = 1 + \gamma M_\infty^2 \text{Sin}^2\,\beta\,(1 - \rho_\infty/\rho) \qquad \text{(shock)} \tag{33}$$

where, for a perfect gas

$$\rho/\rho_\infty = \frac{\gamma+1}{2}\,(M_\infty\,\text{Sin}\,\beta)^2 \Big/ \left[1 + \frac{\gamma-1}{2}\,(M_\infty\,\text{Sin}\,\beta)^2\right] \qquad \text{(shock)} \tag{34}$$

At the body surface, we would like to have $\psi = 0$. This requires (see eqs. (22) and (26) that the origin of coordinates be chosen so that $r_1 = 0$ occur on the stagnation streamline. If this selection can be made, there is no further worry about body surface conditions.

METHOD OF SOLUTION

The solution is found in an inverse manner. The shock curvature is assumed and is twice integrated to find the shock angle and radius. From that, the pressure can be found (eq. (18)). Then on a specified streamline, the entropy is constant at its value on crossing the shock. The state equation and isoenergetic condition (eq. (21)) yield the density, enthalpy and total velocity ($\bar{V}$). Then eqs. (24) and (25) can be solved for the streamline position and flow angle. That completes the solution in the "Mises Space" (ζ, σ, ψ). We return to physical space, finding η, the distance normal to the shock, from the first of eqs. (10). As $\psi = 0$ defines the body, the computed value of η at $\psi = 0$ must be compared to the geometric distance and iterated as necessary. A somewhat more complete description of the program is given in Appendix A.

Implementing the procedure described requires two distinct parts. Once a satisfactory starting solution has been found, one can march downstream. Extrapolate the shock curvature to a new station and proceed exactly as described above.

For the starting solution, a different process is used. An initial distribution of the shock curvature is assumed over a region surrounding the nose. Preferably this is the entire subsonic region (this point will be discussed further later on). This is taken in the form

$$\text{curvature} = a(\sigma) + zb(\sigma) + z^2 c(\sigma) \tag{35}$$

where the most general form for $a(\sigma)$ is

$$a(\sigma) = \frac{\bar{a}}{1 + \bar{b}\ \text{Cos}^2\sigma} \tag{36}$$

Then the solution is constructed for a set of z-stations (typically 8). The solutions at two intermediate stations (say 2 and 5) in two mutually perpendicular (in σ) planes are used to find the values of $\bar{a}$, $\bar{b}$ and the shock standoff distance at the nose. Then the values of $b(\sigma)$ and $c(\sigma)$ are found iteratively by matching the body position and slope at the last (8th) station. Once this starting solution converges, the downstream solution can proceed straightforwardly based on extrapolation of the shock curvature as discussed earlier.

All of the elements described are straightforward and proceed without difficulty except for the iteration involved in determining the initial curvature distribution elements $b(\sigma)$, $c(\sigma)$ in eq. (35).

Originally, the initial distribution was made with $c(\sigma) \equiv 0$ in eq. (35). In that case only the body position was matched (at station 8). For some problems, this appeared to be acceptable and the solution could continue downstream without especial difficulty. It was observed however that the resulting surface values of, say, pressure or Mach number were not smooth but had a bump just downstream of the starting solution. The same behavior had been observed in a code developed for axisymmetric flow. This corresponds to the fact that the body slope is poorly matched at that point and the resulting "corner" generates some mild havoc.

Unfortunately, there was a very large snake in the grass. The problem posed in the present study is not typical of the cases for which the bumpy solution could proceed. On the windward surface of the shuttle vehicle at 65° angle of attack, there is a very extensive sonic or near sonic region. It is not really practical to have the initial solution cover this whole region. Nevertheless, the initial solution can still be found. However one must then march downstream toward the "sonic point". The solution so found is divergent at a critical point near the limiting characteristic separating the sub and supersonic regions. The saddle point behavior is familiar from the method of integral relations to which the present method bears considerable resemblance.

Unless the initial solution is a good one, the solution resists the approach to the critical point with great enthusiasm. Accordingly it became clear that a smooth solution would be needed. For that reason, the third term ($c(\sigma)$ in eq. (35)) was introduced. Then both the body position and slope can be matched at the end of the initial region. For axisymmetric flow, this added term is no great complication and its introduction serves to give good results even when a subsonic region lies downstream. In the present case, the selection of a reasonable iteration procedure becomes of paramount importance. Clearly we cannot perform indefinitely many iterations and hope to have an efficient solution of the problem.

A number of procedures have been tried. First several brute force calculations were made to clarify the expected behavior of $b(\sigma)$ and $c(\sigma)$ when good convergence is obtained on the body position and slope. Next some limited runs were made to get an idea of the precision required in satisfying these matching conditions if the subsequent solution were to proceed without difficulty. These calculations were done for an hemisphere cylinder at $M_{\infty} = 10.0$ and $\gamma = 1.4$ for a perfect gas. Angles of attack of

0, 40 and 50 degrees have been run. The 0 degree case can be compared with similar results from an axisymmetric code. The results agree to within about 1/ 2% for shock shape and surface pressure for the two programs and are in excellent agreement with other calculations. The case serves largely as a check on the overall operation of the present general program. At 50° angle of attack, the windward flow is near sonic for some distance and is, in that sense, typical of the desired shuttle condition. While great improvement was found in calculations using the complete eq. (35), convergence of the iterative process was not good enough. Time did not permit a satisfactory exploration of this vital question. To reduce the sensitivity to sonic behavior somewhat, an angle of attack of 40° was also run. While the iteration scheme which was used contained a strong element of trial and error, the results are gratifying in that reasonable convergence was obtained and it became clear that the solution could continue downstream.

An extended discussion of some of the problems associated with operation is given in Appendix B. Particular attention is directed to the effects of a sonic region.

CONCLUDING REMARKS

The present study has shown that the analysis of three dimensional blunt body flows can be carried out by the method based on approximate integration of the momentum equation across the shock layer. However it is clear that considerable care and more study is required to provide a suitably rapid convergence of the required iterations if an efficient procedure is to be attained. The exploration of such iterations thus far carried out indicates that success is to be expected.

APPENDIX A

The computer program consists of a main program plus eleven subroutines. These are:

NONAX	Main logic program controlling the sequence of use of the subroutines.
CHEM	Does all chemistry calculations for a perfect gas. Could be replaced by real gas
START	Provides initial values at the nose as well as starting estimates of the flow near it.
TEST	Routine to test (and provide an iteration to improve) the starting solution.
SHOKQ(I)	Computes quantities at the shock for specified radius, slope and curvature distribution.
INTEGG(I)	A third order Runge-Kutta routine to integrate the equation for the streamline (eqs 24 and 25) (one step for each streamline).
AITKEN	Interpolation routine for use in INTEGG
TRAN(I)	Transfer the results of INTEGG from the ζ, σ, ψ coordinates to z, θ, η ones and integrates the first of eqs (10) to find η.
CROS(I)	Tests the position of the body from TRAN against the actual geometric coordinates and provides an iteration scheme.
EXTRAP	Extrapolates the solution one step downstream when the results in CROS converge.
EXTEND	Routine to extrapolate a small distance into the separated leeside region.
SMOOTH	A least squares smoothing routine to smooth the shock estimates so that two lateral derivatives can be found.

A listing of these routines is not presented (although available) because their present form contains a confusing number of logic elements associated with various iteration procedures which will have no part in a final program. However the general sequence is to make an initial estimate of the shock slope and position (START), use that to find shock values for 5 stations (SHOKQ), integrate the streamline equations (INTEGG) and transform to physical space (TRAN) and test the result (TEST, CROS) to determine an acceptable nose curvature distribution (eq (36)). Then one goes through INTEGG, and TRAN to station 8, uses CROS (8) to test the body position and slope at station 8. Once that converges the solution is extrapolated (EXTRAP) and one goes thru SHOKQ, INTEGG, TRAN and CROS, interating as necessary.

Appendix B.

This section discusses some of the details of the agonies connected with getting the program to run and is in the nature of a status report on its present imperfect condition.

First of all, all of the subroutines which compute the consequences of an assumed shock curvature distribution (starting routine) or extrapolation (downstream continuation) are satisfactory. These comprise the construction of the shock slope and radius, evaluation of quantities behind the shock (SHOKQ) and hence the pressure distribution, integration (INTEGG) of the equations for the streamline and flow direction (Eqs. 24 and 25), transformation of these results to σ = const lines and integration of eq. (10) to find η and thus return to physical space (TRAN) and then to compare (CROS) the body coordinates thus generated with the actual ones found geometrically.

The operating status and attendant problems can be seen with the aid of figs. 2 and 3. These give the shock shape, and surface pressure and Mach number distribution for an hemisphere cylinder solved for a perfect gas at M = 0 and γ = 1.4. In figure 2 the angle of attack is 40°. In this case the starting solution applies to station 8 and yields a solution to that point which is entirely supersonic and which involves only the spherical nose of the body so that the starting solution remains axisymmetric with respect to the wind directions. In that case the starting solution is one in which the body position is matched at station 8 correct to $\Delta\eta$ = .004 (out of .18)

while the slope is 3% below the geometric value. The subsequent downstream calculation proceeds without any difficulty about convergence (a maximum of 3 iterations per station). The calculation was halted arbitrarily, not because of any operational problem. For future discussion, the results on the windward streamline should be noted. The shock surface pressure and surface Mach number vary smoothly and, importantly, the surface Mach number is about 1.2. Off the surface (not shown) the values are larger; increasing monotonically toward the shock.

Now consider figure 3, which shows corresponding results for $\alpha = 50^{\circ}$. In this case, the starting solution covers a small portion of the cylindrical afterbody. As before, at Station 8, the solution has position correct to $\Delta\eta = .005$. (out of .18).

The error in slope is about 7% on the windward streamline. There was no problem with the solution to this point. On marching downstream the solution (fig. 3) has no unusual features over any but the windward part of the body. Except for that region, the results are as one would expect as one proceeds from $\alpha = 40^{\circ}$ (fig. 2) to $\alpha = 50^{\circ}$.

However, on the wind side there is trouble. The solution found is as indicated, with, in particular, the Mach number on the windward streamline becoming subsonic and falling to relatively low values. Under these circumstances the error criterion on $\Delta\eta$ (body position) was never satisfied at stations 11 or 12 (for $\theta = 90, 85$). The program accepted this solution when no improvement occurred after several iterations.

The principal difference between the $\alpha = 40$ and 50 cases is the indication in the latter case of a local near sonic region. It has been shown

in other analysis (ref. 7 and this author's unpublished work) that the present method is much like that of integral relations in that the problem is singular near a "sonic" region. This arises because (eq. 10), the changes in the value of η with changes in the shock geometry have an effective influence coefficient roughly proportional to a weighted integral of (M^2-1) across the shock layer. In two dimensional or axisymmetric flow this behavior is very straightforward and clear; in three dimensions the consequences are rather obscure. In any case, there is danger.

This describes the status and raises some specific questions which can be examined in turn. These include:

1. Is there a fundamental problem due to violation of required characteristic propagation directions?
2. Is the solution sensitive to the position of Station 8?
3. Must the slope in the starting solution (Station 8) be matched much more accurately than at present?
4. Is there a local "sonic" region which can be "jumped"?
5. Is the solution, in fact, correct?
6. What is the effective way to iterate b, c (eq. 35)?
7. Do we require a body with continuous curvature?

At the present time, none of these questions can be resolved entirely, but some indications are available. The questions about propagation of shock effects toward the body is not a local error. In the present case, one really

has the shock affect propagated normal to the shock and hence nearly normal to the body which, from the viewpoint of characteristics is most valid if M is near 1. Actually the local shock effect propagated is rather diffuse since we specify the shock by its curvature; that is, we in effect require it to be twice differentiable. There seems to be no unusual error due to this behavior, and if anything the near sonic regions are most realistically portrayed in this respect.

The sensitivity of the results to the specified position of Station 8 (Question 2) has not really been examined. A few runs have been made (at low angle of attack) with that station moved aft about 10%. The results were unchanged. No other tests have been run to date. It should be noted however that in the $\alpha = 50$ case (fig. 3), the entire flow at Station 8 was supersonic. It was not just the "average" value.

The question (#3) of the effect of slope errors is less clear. In the particular run given in figure 3 the error in position and slope is as sketched below. In particular, the two errors are in a direction to tend to compensate each other on going to Station 9. This would then require recompression in going to Station 10.

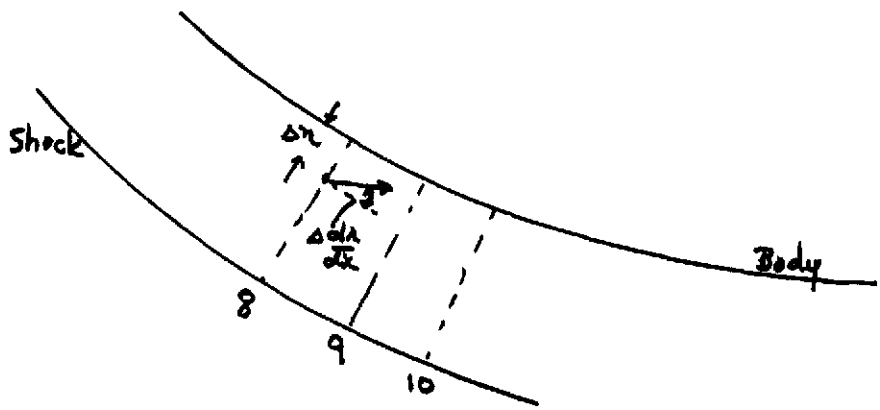

Errors at Station 8 (Exaggerated)

This brings us to question 4. If there is a real "near sonic" region, can one jump over it or is it too extensive for a meaningful jump? This question is, in the end, related to question (5); what is the real answer? No other results appear to be available. However it seems pretty unlikely that the result of figure 3 is correct at least so far as it shows a large drop of the Mach number (to .80 at Station 12) on the windward streamline.

Question 6 was discussed earlier in the main text. It may be that one can iterate (b) generally but only require that (c) match formally at a few points. This remains open.

Finally, the body tested has discontinuous curvature at the juncture of the spherical nose and cylindrical afterbody. Such a jump is a frequent source of difficulty with flow fields and is usually resolved by a fillet at the juncture forcing continuous curvature. In the present analysis this may not be a problem because of the relatively large step size (about 10% of the nose radius) in that region. It should be noted however, that the surface pressure irregularities in the computed examples (figs. (2) and (3)) occur at about the juncture of the nose and afterbody.

REFERENCES

1. Maslen, S. H.: Inviscid Hypersonic Flow past Smooth Symmetric Bodies. AIAA J., Vol. 2, pp. 1055-1061, 1964.

2. Jackson, S. K.: The Viscous-Inviscid Hypersonic Flow of a Perfect Gas over Smooth Symmetric Bodies. Ph. D. thesis, U. of Colorado, 1966. Available from University Microfilms, Ann Arbor.

3. Perini, L. L. and Melnik, W. L.: Nonequilibrium Flow Past Smooth Symmetric Bodies, J. Space Rockets, Vol. 5, N. 3, pp. 308-312, March 1968.

4. Olstad, W. B.: Nongray Radiating Flow about Smooth Symmetric Bodies. AIAA J., Vol. 9, N. 1, pp. 122-130, January 1971.

5. Grose, W. L.: A Thin Shock Layer Solution for Nonequilibrium Inviscid Hypersonic Flows in Earth, Martian, and Venusian Atmospheres. NASA TN D-6529, 1971.

6. Maslen, S. H.: Asymmetric Hypersonic Flow. NASA CR-2123, 1972.

7. McDonald, L. L.: Calculation of Inviscid Hypersonic Flow Fields Over Blunt Bodies. Masters Thesis, North Carolina State University, 1973.

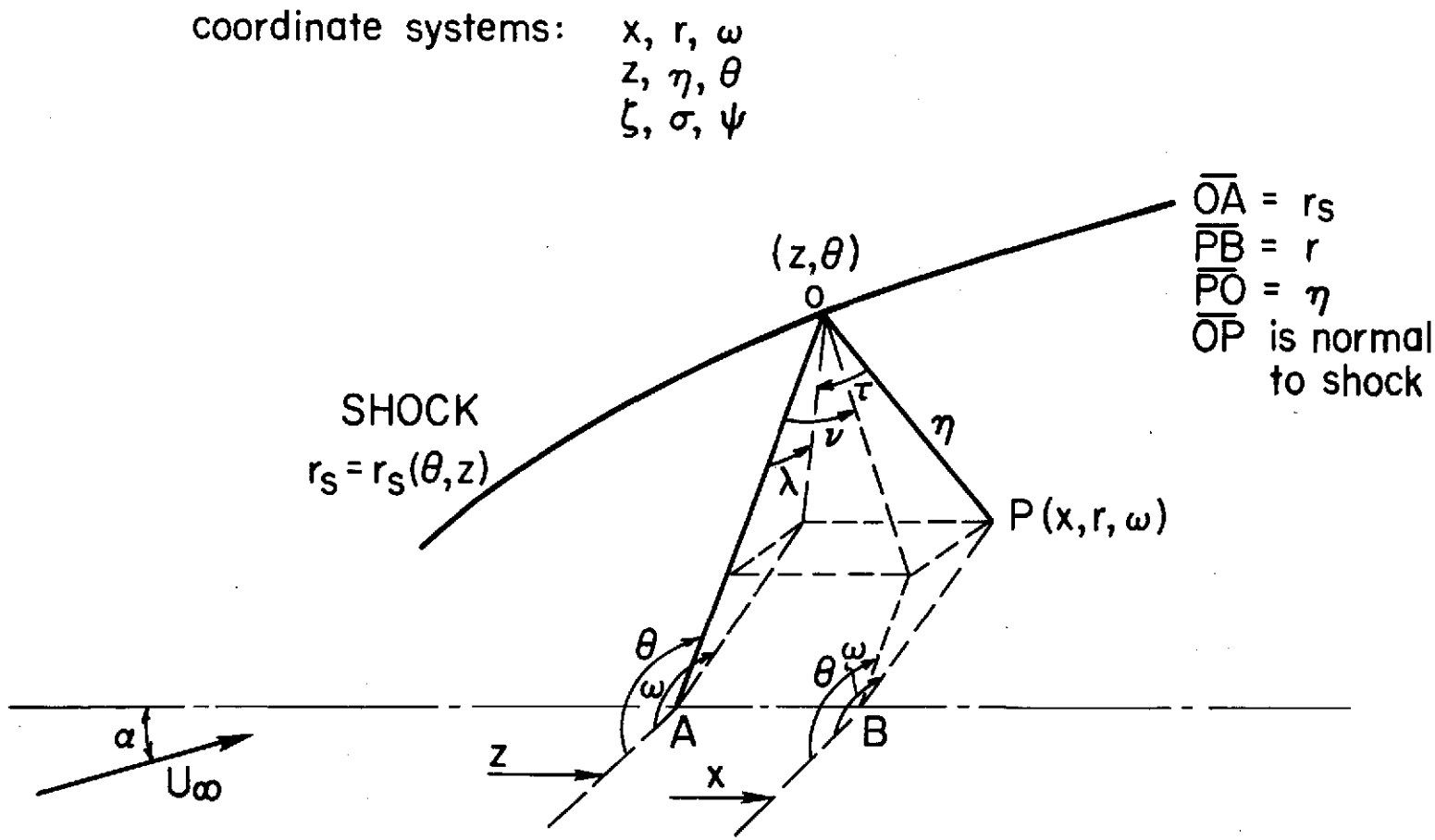

Fig. 1. Coordinate Systems

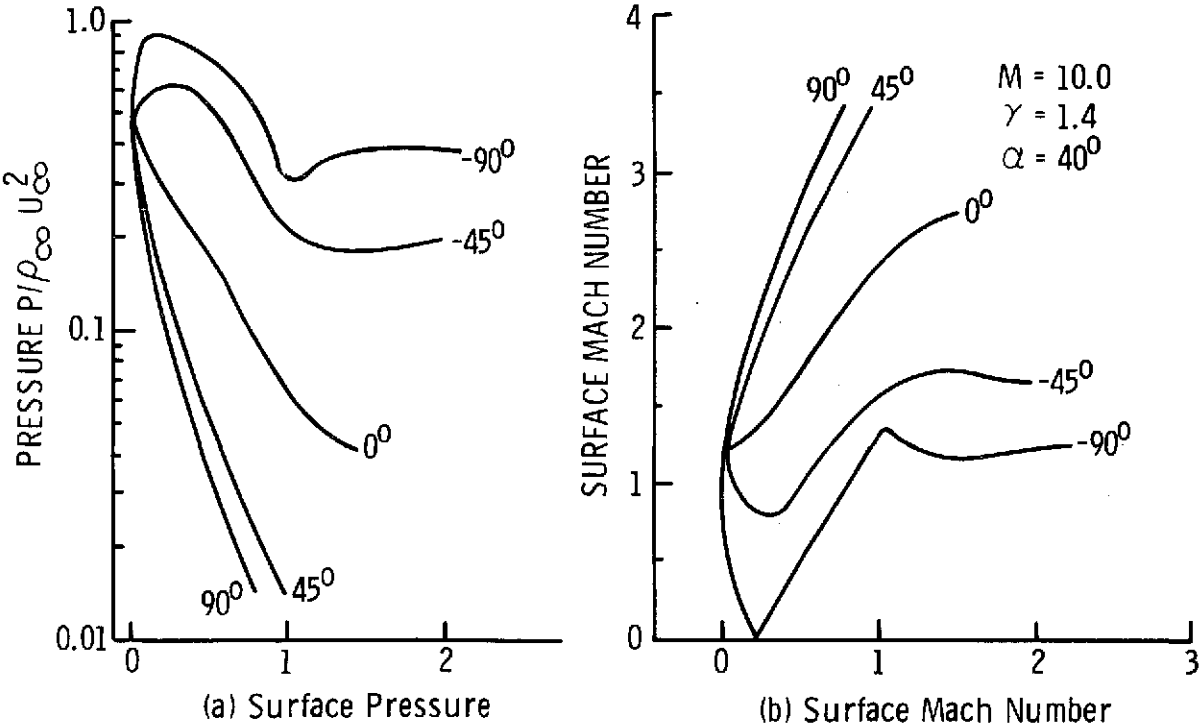

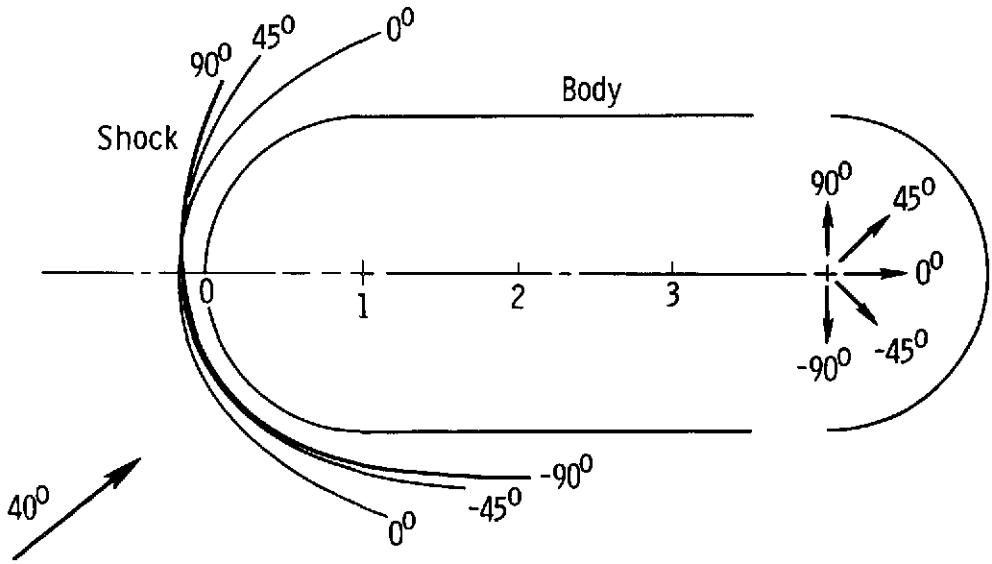

(c) Shock Shape

Fig. 2. Shock Shape and Surface Pressure and Mach Number for Hemisphere Cylinder ($\alpha = 40^{\circ}$).

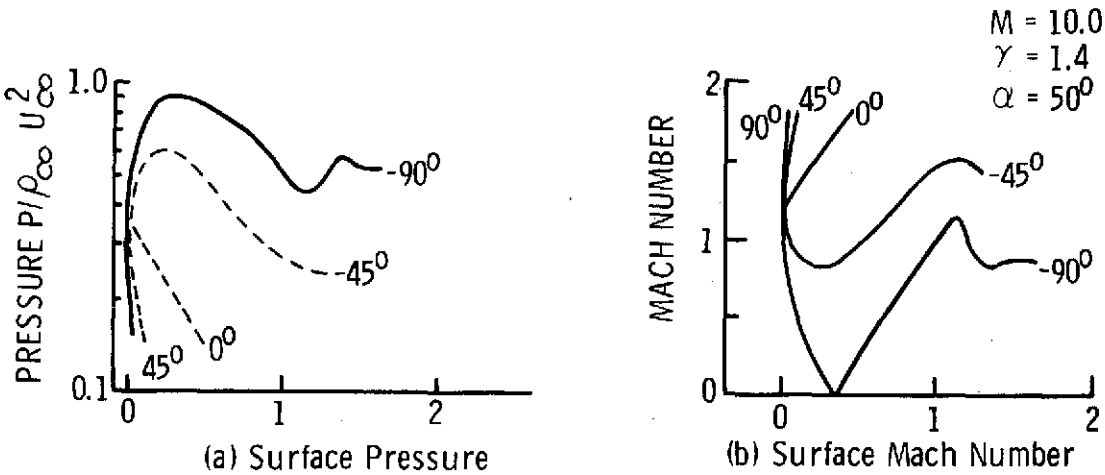

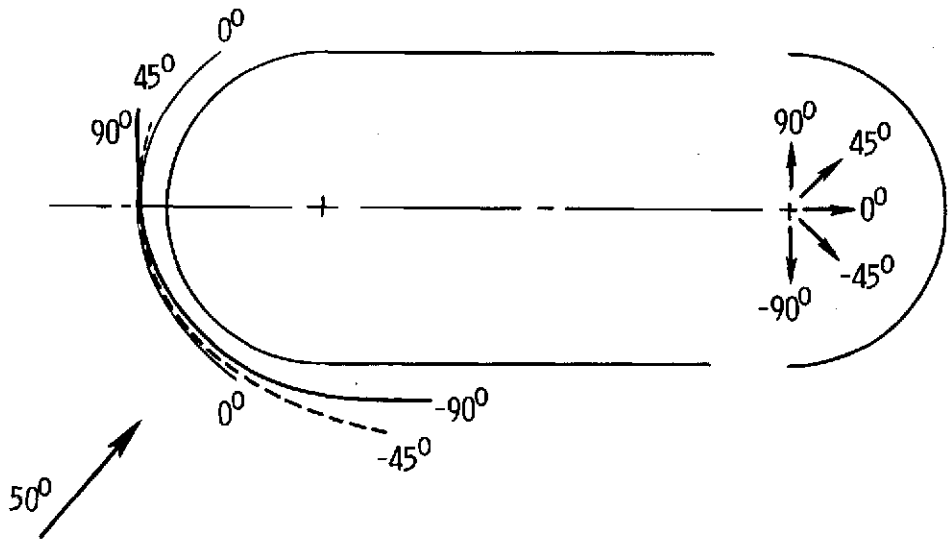

(c) Shock Shape

Fig. 3. Shock Shape and Surface Pressure and Mach Number Distribution for Hemisphere Cylinder ($\alpha = 50^{\circ}$).